JOURNAL OF MATERIALS SCIENCE 21 (1986) 2819–2824

A natural wear resistant material

M. K. AGHAJANIAN, E. BREVAL, J. S. JENNINGS, N. H. MACMILLAN
Materials Research Laboratory, The Pennsylvania State University, University Park, Pennsylvania 16802, USA

A study has been made of Danto Koruntz (Danto International Ltd.), a natural material now beginning to find use in wear applications. Its microstructure is described and its density, coefficient of thermal expansion, thermal conductivity, hardness, elastic constants, flexural strength, fracture toughness and work of fracture are reported. Compared to a typical man-made 95% dense sintered wear alumina, which is somewhat harder and tougher and considerably stronger and stiffer, Danto Koruntz is much less erosion resistant and exhibits qualitatively different thermal shock behaviour. When slid on itself, Danto Koruntz exhibits a slightly lower coefficient of friction than does the alumina.

1. Introduction

One consequence of the present lack of fundamental understanding about wear is the great diversity of materials employed in any given wear application. Pipes used in pneumatic or slurry conveyance, for example, are variously made of plain carbon steel, high alloy cast iron or wooden staves; and those made of steel may be used either unlined or lined with polyurethane, rubber, Al_2O_3, SiC or fused-cast basalt. A recent addition to this pantheon of wear-resistant materials is Danto Koruntz, a fine grained quartzo-feldspathic gneiss from Mount Danto in Japan, which is intended to be used as-quarried. The present paper describes the structure of Danto Koruntz and compares various of its mechanical and physical properties, its wear behaviour, and its thermal shock resistance with those of a 95% dense sintered alumina which is widely used in wear applications.

2. Structure

At the macroscopic (decimetre) scale, Danto Koruntz is a uniform, light grey rock which is free of obvious cracks and pores. However, it is not completely isotropic, for it contains stringers of darker-coloured minerals aligned more or less parallel to one direction. These stringers are typically of centimetre length and millimetre width. Figs 1a and b show rough polished (600 grit SiC) sections oriented parallel and perpendicular to these stringers. For later reference, the direction parallel to the stringers is designated as the z-axis, O_z; and x and y axes, O_x and O_y, are defined as arbitrary orthogonal directions in the plane perpendicular to O_z.

Table I gives the overall chemical compositions of Danto Koruntz, as determined by wet chemical methods, and the alumina, as supplied by the manufacturer. X-ray diffraction and polarized light microscopy reveal that most of the SiO_2 in Danto Koruntz is present as quartz. This phase constitutes about 80% of the rock. The remaining 20% includes various feldspars, micas (biotite and sericite), pyroxenes and amphiboles, plus garnet and assorted opaque minerals.

Figs 2a and b, which are oriented perpendicular to O_z and O_x, respectively, both show equiaxed grains ranging in size from 10 to 1000 μm. In general, the quartz grains are $\gtrsim 50\,\mu$m and the minor constituents make up the bulk of the smaller grains. The similarity between Figs 2a and b shows that the anisotropy visible in the macrostructure, Figs 1a and b, does not persist at the microstructural level; and the X-ray diffraction studies confirm that the quartz grains exhibit no preferred orientation. The failure of attempts to vacuum impregnate Danto Koruntz with brightly coloured resin demonstrate a complete absence of interconnected porosity, and the optical microscopy studies show that it contains neither isolated pores nor microcracks. The microstructure of the alumina, which consists of $\sim 10\,\mu$m equiaxed grains of α-Al_2O_3 bonded together by a glassy SiO_2-based grain boundary phase [1] and which contains a few isolated pores, is shown in Fig. 3. This alumina exhibits no preferred orientation and appears to be isotropic.

3. Mechanical and physical properties

Table II compares various of the mechanical and physical properties of Danto Koruntz and the alumina. Density was determined by weighing and measuring rectangular blacks, and thermal expansion α and thermal conductivity k were measured with a Harrop TD-716 Thermal Dilatometer (Columbus) and a Colora Thermoconductometer (Württemberg),

TABLE I Chemical composition (wt %)

Constituent	Danto Koruntz	Alumina
SiO_2	82.8	2.63
Al_2O_3	8.72	96.00
TiO_2	0.27	–
K_2O	2.99	–
Na_2O	2.23	0.04
Fe_2O_3	1.08	–
CaO	0.69	0.66
MgO	0.24	0.66
MnO	0.025	–
Ignition loss	0.89	–

0022–2461/86 $03.00 + .12

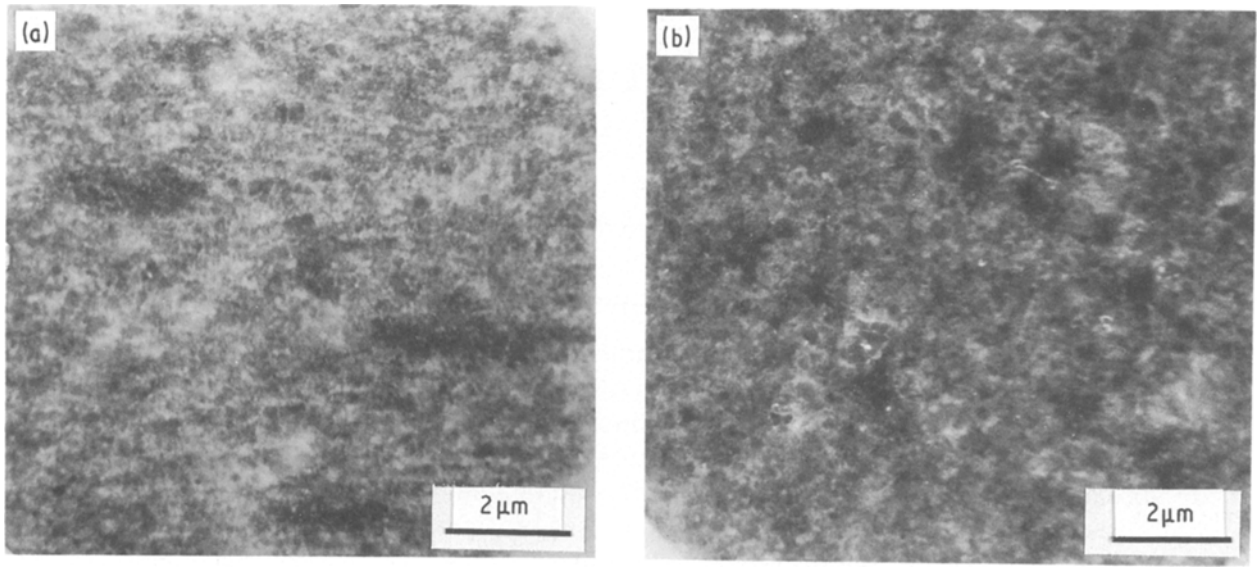

Figure 1 Rough polished surfaces of Danto Koruntz oriented (a) parallel and (b) perpendicular to the stringers of darker coloured minerals.

respectively. The dilatometric measurements were made over the temperature range 300 to 1300 K, and the thermal conductivity was determined as the average over the temperature interval 360 to 373 K. Note that Danto Koruntz has a density close to that of α-quartz (2650 kg m^{-3}) and so is about one third less dense than the alumina, which has a density (3750 kg m^{-3}) $\sim$ 0.94 times that of sapphire (3970 kg m^{-3}).

Young's modulus E was measured at room temperature along an arbitrary direction in the alumina and along O_x, O_y, and O_z in Danto Koruntz by the sonic resonance (standing wave) technique [2], using flexural modes of vibration. In Danto Koruntz, E was found to vary with orientation by $< 10\%$, being lowest along O_z (i.e. parallel to the dark-coloured stringers) and highest along O_y. Along both O_x and O_y, E is slightly higher when the flexural displacement occurs parallel rather than perpendicular to the stringers. The shear modulus G was determined for both materials by the torsional variation of the same technique. In neither case did G show any significant variation with orientation. For both shear and uniaxial tensile or compressive modes of deformation, the alumina is about six times as stiff as Danto Koruntz. An approximate value of 0.14 was obtained for Poisson's ratio ν of Danto Koruntz by averaging E over all orientations and using the relationship $E = 2G(1 + \nu)$ from isotropic elasticity theory. This value is much lower than Poisson's ratio of the alumina (0.24).

Vickers hardness was measured with a Leitz Miniload Tester, using loads of 1 N (Danto Koruntz) or 20 N (alumina) and a loading time of 10 sec. In the case of Danto Koruntz, the load adopted was the maximum consistent with keeping the indentation within a single quartz grain and avoiding microchipping. It was not possible to measure the hardness of individual grains of the minor constituents because of their small size. A few measurements were made which covered several such grains, and these exhibited great scatter. It is clear that the minor constituents of Danto Koruntz vary greatly

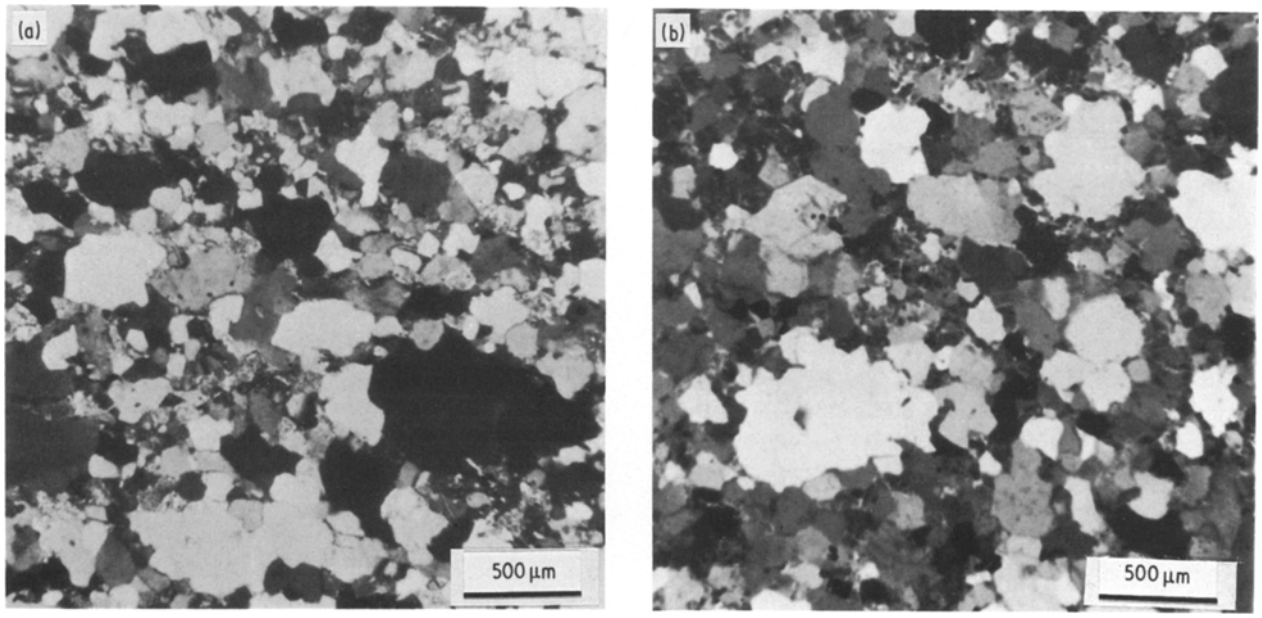

Figure 2 Thin sections of Danto Koruntz oriented (a) parallel and (b) perpendicular to the stringers of darker coloured minerals. The large equiaxed grains are quartz. Polarized light microscopy, crossed nicols.

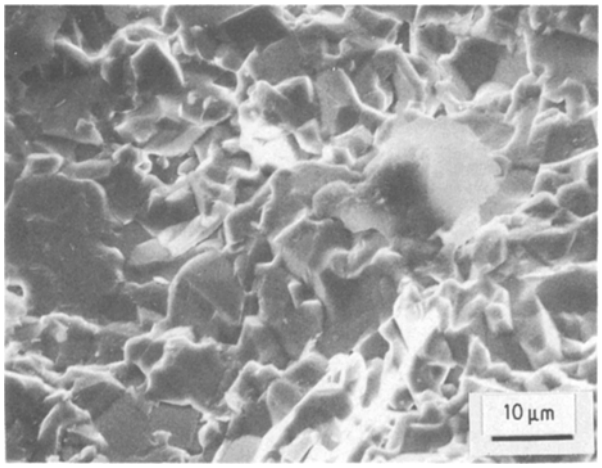

Figure 3 Fracture surface of the alumina showing ~ 10 μm equiaxed grains of α-Al_2O_3 and occasional pores. The fracture occurs along the grain boundaries.

in hardness. In the case of the alumina, each indentation covered several grains. The hardness is about 30% greater than that of the quartz constituent of Danto Koruntz.

Flexural strength σ was measured on an Instron Universal Testing Machine in three point bending at room temperature. The test jig had a span of 2.54 cm between the two outer supports and the crosshead speed was 8.3×10^{-5} cm sec^{-1}. The alumina specimens were plates 1.5 mm thick, 5.5 mm wide and about 30 mm long, and the Danto Koruntz specimens were plates 3 mm thick, 10.5 mm wide and about 30 mm long. In both cases the tensile surface was polished with diamond pastes down to 1 μm on kerosene covered paper. The alumina proved to be a full order of magnitude stronger than Danto Koruntz, which latter exhibited little anisotropy of strength. There is some indication in the data that Danto Koruntz is a few per cent weaker when it fractures in a plane perpendicular rather than parallel to the dark coloured stringers.

The plane strain mode I, fracture toughness K_{IC} and the work of fracture G_{IC} were measured for both materials by the double torsion technique. The specimens were plates, each of which had a central groove ~ 0.75 mm wide machined along its tensile face. The depth of this groove was 0.5 times the thickness of the plate, and it was notched at the loaded end to initiate fracture. In the case of the alumina the plates were 1.27 cm wide, 1.5 mm thick, and 4 to 5 cm long; and for Danto Koruntz some plates were 1.9 cm wide, 2.7 mm thick and 6.5 cm long and the others were 2.4 cm wide, 3.3 cm thick and 7.0 cm long. The tests were carried out on the same Instron at the same crosshead speed of 8.3×10^{-5} cm sec^{-1}, and the compliance was calculated from the dimensions of the specimen and the measured values of Young's modulus. K_{IC} was independent of orientation for both materials, and was ~ 2.5 times larger for the alumina than for Danto Koruntz. There was much less difference in work of fracture between the two materials due to the much lower Young's modulus of Danto Koruntz.

4. Friction and wear behaviour

The coefficient of friction was measured for both materials in air of approximately 50% relative humidity at room temperature, using a reciprocating flat-on-flat test geometry. This involved sliding a 9 mm diameter disc backwards and forwards on a 17 mm diameter disc under a nominal normal stress (load divided by nominal area of contact) of 15 kPa. The sliding velocity was 0.3 mm sec^{-1}, and the amplitude of the motion was 5 mm. Both surfaces were initially polished with diamond pastes down to 1 μm on kerosene covered paper, and the coefficient of friction μ_f was recorded after 1 h (~ 120 cycles) of sliding. For Danto Koruntz,

TABLE II Mechanical and physical properties of Danto Koruntz and sintered alumina

Property	Material	
	Danto Koruntz	Alumina
Density (kg m^{-3})	2600 ± 10	3750
Thermal expansion (10^{-6} K^{-1})	23(293–773 K) (as quarried) 14(293–773 K) (after heating to 1193 K)	10.6 (373–1273 K)
Thermal conductivity (Wm^{-1} K^{-1})	3.32	23.9
Young's modulus (GPa)	‖ x 55.1* 56.8† ‖ y 58.6† 57.0* ‖ z 54.2* 54.5*	326 ± 4
Shear modulus (GPa)	in yz plane 24.4 in zx plane 24.7 in xy plane 24.3	132 ± 1
Poisson's ratio	0.14	0.238 ± 0.014
Vickers hardness (GPa)	11.4‡ (quartz), 5–9‡ (other constituents)	14.6 ± 1.6§
Flexural strength (MPa)	tension ‖ x, load ‖ z 25.7 ± 1.1 tension ‖ y, load ‖ x 27.8 ± 1.5 tension ‖ z, load ‖ y 27.1 ± 1.3	301 ± 25
Fracture toughness (MPa m$^{1/2}$)	1.47 ± 0.07	3.84 ± 0.12
Work of fracture (Jm^{-2})	37.1	42.5

*Displacement perpendicular to the dark-coloured stringers.
†Displacement parallel to the dark-coloured stringers.
‡1 N load.
§20 N load.

μ_f ranged between 0.13 and 0.15, regardless of orientation, and for the alumina it was 0.19. Neither material showed appreciable wear as a result of the experiment.

Measurements of the resistance of Danto Koruntz and of the alumina to solid particle erosion were made with a whirling-arm apparatus developed in this laboratory [3]. This apparatus created a continuous vertical screen of falling particles by endlessly recirculating 400 g of 600 μm equiaxed angular WC–8 wt % Co particles through a constrictive orifice at a constant mass flow rate of 12.5 g sec^{-1}. In addition it repeatedly drove 12.7 mm diameter disc-shaped specimens mounted on the ends of the whirling arm through this screen to erode them. The impact velocity, defined as the vector sum of the vertical velocity of the falling particles and the horizontal velocity of the end of the whirling arm, was maintained constant at 4 m sec^{-1}. The impact angle was varied from 15° (glancing incidence) to 90° (normal incidence) by mounting each specimen on the whirling arm at a different angle to the impact velocity vector.

Mass loss against time of erosion at normal incidence is shown in Fig. 4, revealing that Danto Koruntz erodes several times faster than the alumina. The data points and error bars along the curve for Danto Koruntz indicate the mean and the extreme (maximum and minimum) mass losses obtained from six specimens, two of which were oriented perpendicular to each of the axes O_x, O_y, and O_z. There was no consistent variation of mass loss with orientation. Fig. 5 shows the variation with impact angle of the steady state erosion E, defined as

$$E = \frac{1}{n}\frac{\partial M}{\partial N_i} \quad (1)$$

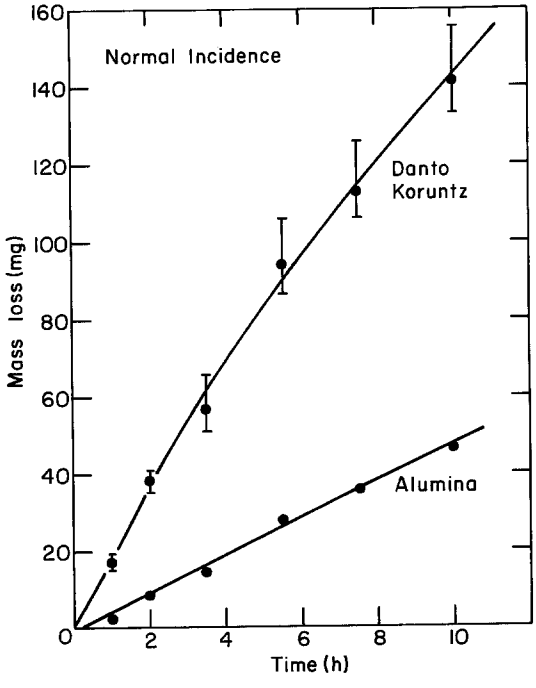

Figure 4 Mass loss against time of erosion for Danto Koruntz and the alumina. The impact angle and velocity were 90° and 4 m sec^{-1}, and the erosive particles were 600 μm angular chunks of WC–8 wt% Co. For Danto Koruntz both the mean and the extreme mass losses obtained from six specimens of varying orientation are shown.

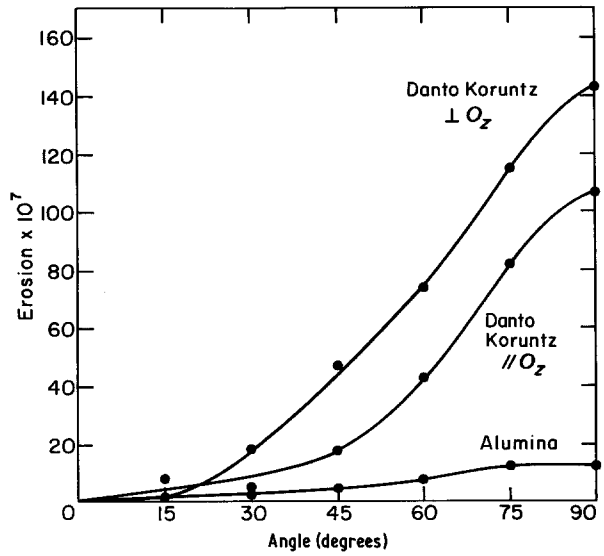

Figure 5 Steady state erosion against impact angle for Danto Koruntz and the alumina. The erosive particles and the impact velocity were the same as in Fig. 4. The difference between the curves for the differently oriented specimens of Danto Koruntz is probably not significant.

where m is the average mass of an erosive particle and M is the mass loss due to a number N_i of erosive impacts large enough that $\partial M/\partial N_i$ is constant (i.e. the mass loss curve of Fig. 4 is a straight line). Both materials show the angular dependence of erosion characteristic of a brittle material [4], but Danto Koruntz erodes several times faster than the alumina at all impact angles. The disparity increases as the impact angle increases. The difference between the curves in Fig. 5 for Danto Koruntz specimens oriented parallel and perpendicular to the dark-coloured stringers (O_z) is probably not significant.

Fig. 6 shows the surfaces of specimens of both materials which have been eroded at the impact angles indicated until steady state conditions were achieved. In the case of Danto Koruntz eroded at normal incidence the total depth of material removed was ~ 500 μm (i.e. about the diameter of the largest quartz grains), while for the alumina the depth removed at the same angle (~ 100 μm) was ~ 10 times the grain size. At 30°, the depths of removal were ~ 70 and ~ 20 μm, respectively. At normal incidence the alumina appears to erode by a mixture of intragranular and intergranular fracture. Sub-micrometer size pieces are chipped off the individual grains until their remaining parts are removed by intergranular fracture. In contrast, the impacts of the erosive particles at 30° produce what appears to be a thin surface layer of plastically deformed material but may actually be a mass of small wear particles cold-welded together. This layer occasionally spalls away to expose conchoidal (intragranular) fracture surfaces. In the case of Danto Koruntz, something of the same trend is apparent, though the appearances of the eroded surfaces are complicated by the macrostructural heterogeneity visible in Figs 1a and b. The surface of the specimen eroded at 90° is rougher than that of the specimen eroded at 30°, and it exhibits evidence of (i) conchoidal intragranular fracture (chipping) of the quartz constituent over most of its area and (ii) occasional removal of material (presumably the minor

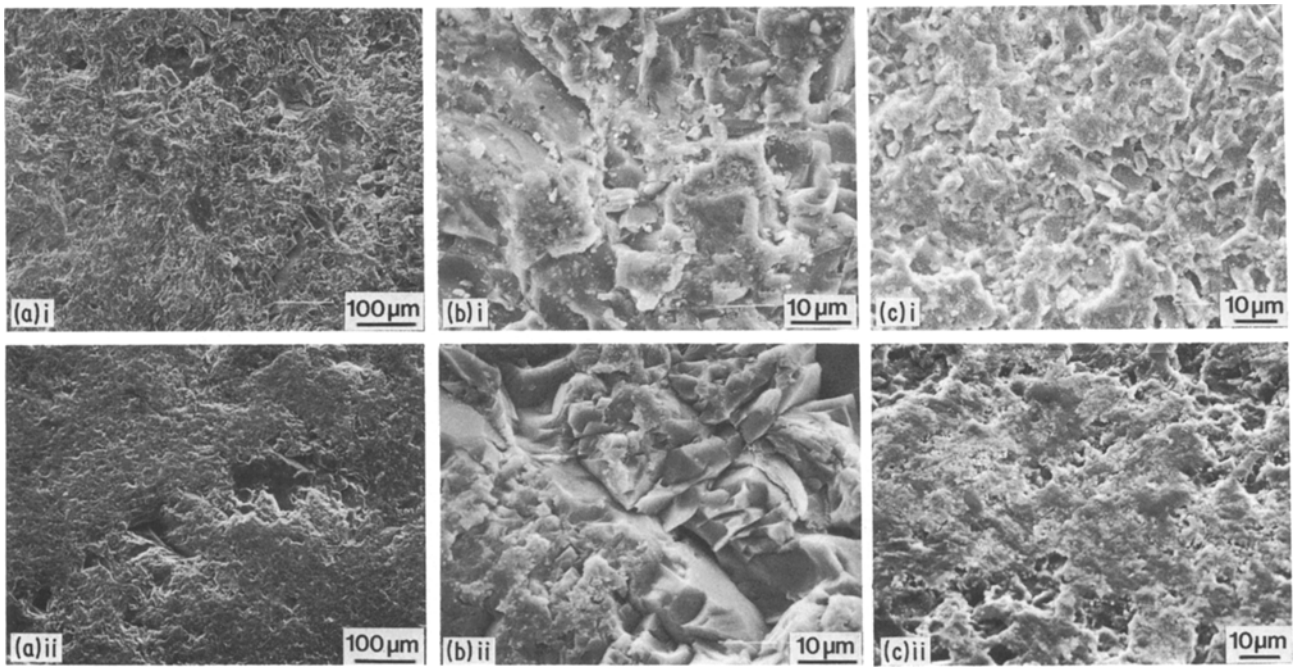

Figure 6 Steady state erosion surfaces of (a, b) Danto Koruntz and (c) the alumina at impact angles of (i) 90° and (ii) 30°.

constituents) by intergranular fracture. On the surface of the specimen eroded at 30°, the debris appears to be more adherent over most of the area; and where the debris layer has detached the exposed fracture surface exhibits evidence of intergranular rather than intragranular failure. It is presumed that the adherent debris is mostly quartz and that the holes in this layer develop where the minor constituents are concentrated. When these spall away by intergranular fracture, the underlying quartz is exposed.

5. Thermal shock behaviour

The thermal shock behaviour of Danto Koruntz and the alumina was determined by a quenching technique. Bend specimens were equilibrated at different temperatures in air and then quenched into water at room temperature (298 K) before being tested in three-point bending at a crosshead speed of 8.3×10^{-5} cm sec^{-1}. The specimens were 3.8 mm thick, 5.7 mm wide and 30 mm long; and they were polished on their tensile surfaces using diamond pastes down to 1 μm on kerosene covered paper. In the case of Danto Koruntz, the dark-coloured stringers were parallel to the length of the bar and the loading direction was O_y.

Table III lists the first, second and fifth thermal shock parameters [5]

$$R = \sigma(1 - \nu)/E\alpha \quad (2a)$$

$$R' = k\sigma(1 - \nu)/E\alpha \quad (2b)$$

$$R'''' = K_{IC}^2/\sigma^2(1 - \nu) \quad (2c)$$

TABLE III First, second and fifth thermal shock resistance parameters

	R (K)	R' (kWm^{-1})	R'''' (m)
Danto Koruntz	18.8	0.06	3.42×10^{-3}
Alumina	55.6	1.3	0.30×10^{-1}

for both materials as calculated from the data listed in Table II. R represents the largest temperature drop that a semi-infinite ceramic body can withstand without cracking when subjected to an infinitely fast quench (i.e. when the heat from the quenching medium is transferred instantly to the surface of the body but is not conducted into the bulk). In practice, of course, some conduction does occur, and it is better to take the effects of thermal conductivity into account. R' is designed to do this. It is a measure of the maximum steady state heat flow that the ceramic can withstand. R and R' are derived from stress criteria of failure and assess resistance to fracture initiation. R'''', in contrast, is a measure of resistance to crack propagation. It is an inverse measure of the total length of through-crack that can be formed in a unit area of a surface layer (of unit thickness) by the strain energy stored in a unit area of that layer when fracture is initiated. Higher values of R'''' indicate greater thermal shock resistance (i.e. that less total damage will occur once the critical temperature drop ΔT_c needed to initiate fracture is exceeded). Note that R'''' is a measure of the total amount of damage done rather than of the consequent reduction in strength. The residual strength is lower when a single flaw propagates into a single large crack than when many flaws grow into many smaller cracks.

The residual bend strengths of Danto Koruntz and the alumina after quenching from different temperatures are shown in Fig. 7. The alumina behaves like a typical high strength engineering ceramic [6]. For temperature drops $\Delta T < \Delta T_c$ pre-existing flaws do not extend and the residual strength remains constant. However, when $\Delta T = \Delta T_c$, sudden rapid crack propagation occurs, leading to catastrophic loss of strength. The new long cracks are sub-critical in the stress field generated by the temperature drop ΔT_c, so ΔT must increase to ΔT_f before they begin to propagate again. As a result a short plateau exists in

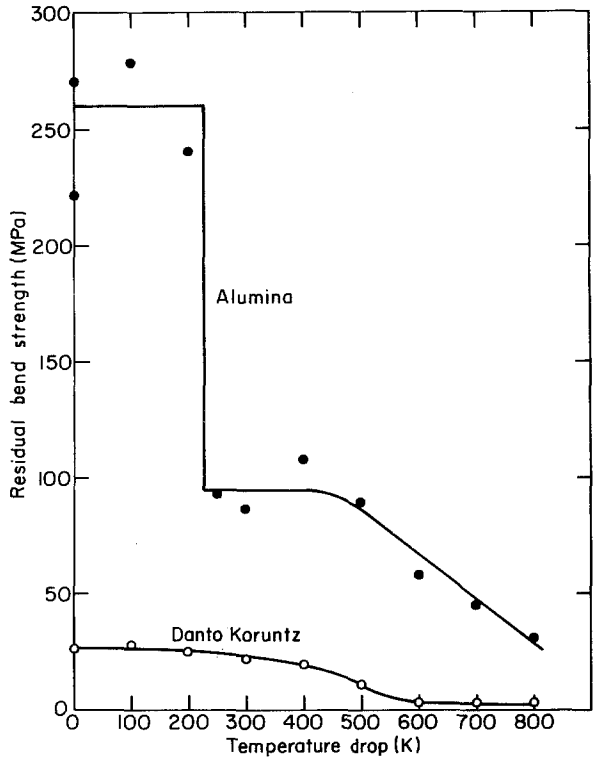

Figure 7 Residual bend strength of Danto Koruntz (○) and the alumina (●) after quenching from different temperatures into water at 298 K.

the residual strength data for the alumina. The residual strength is independent of ΔT in the range $\Delta T_c < \Delta T < \Delta T_f$. As ΔT exceeds ΔT_f further crack growth occurs to a length that increases monotonically with ΔT, resulting in a gradual decrease in residual strength. In contrast, Danto Koruntz exhibits the gradual decrease in residual strength typical of a weaker ceramic [6]. The decrease is gradual because there is only a limited amount of elastic energy available in the quenched body when crack initiation occurs. This results in stable crack propagation to a final length that is a monotonically increasing function of ΔT.

6. Conclusions

Compared to a typical man-made high strength wear alumina, Danto Koruntz is an order of magnitude weaker and six times more compliant at room temperature. Its hardness and toughness at that temperature are only $\sim 80\%$ and $\sim 40\%$ of the corresponding values for the alumina. As a result, it exhibits substantially lower resistance to erosion by solid particle impact at low velocities and qualitatively different thermal shock behaviour. Despite the fact that the alumina exhibits a 60% drop in strength when quenched through a temperature interval $\gtrsim 200$ K, the initial difference in strength is so large that the alumina retains greater residual strength than Danto Koruntz even after quenching through a drop of 900 K.

References

1. N. H. MACMILLAN, *Amer. Ceram. Soc. Bull.* **59** (1980) 697.
2. S. SPINNER and W. E. TEFFT, *ASTM Proc.* **61** (1961) 1221.
3. M. GRIFFIN, MS thesis in Solid State Science, The Pennsylvania State University, 1985.
4. C. M. PREECE and N. H. MACMILLAN, *Ann. Rev. Mater. Sci.* 7 (1977) 95.
5. J. NAKAYAMA, in "Fracture Mechanics of Ceramics". Vol. 2: "Microstructure, Materials and Applications", edited by R. C. Bradt, D. P. H. Hasselman and F. F. Lange, (Plenum Press, New York, 1973) p. 759.
6. R. W. DAVIDGE, "Mechanical Behavior of Ceramics", (Cambridge University Press, Cambridge, 1979) p. 118.

Received 6 September
and accepted 4 October 1985